Pak. J. Statist.
2026 Vol. 42(2), 129-156

MODELLING THE MORTALITY RATE OF COVID-19 PATIENTS WITH A NOVEL EXPONENTIATED PARETO INVERSE EXPONENTIAL DISTRIBUTION

Ibrahim Sule[1§] and **Mogiveny Rajkoomar**[2]
Department of Information Systems, Faculty of Accounting and Informatics
Durban University of Technology, Durban, South Africa
Email: [1]sulei@dut.ac.za; [2]mogier@dut.ac.za
[§]Corresponding author

ABSTRACT

Probability distributions are vital tools in proper interpretation of epidemiological data, such as patient survival times, recovery periods, and mortality rates which is essential for public health planning, resource allocation, and evaluating the success of interventions. By integrating the characteristics of the Pareto and inverted exponential distributions into an exponentiated framework that can describe COVID-19 datasets, this study presents a novel three-parameter exponentiated Pareto inverted exponential distributions. This novel model extends the classical inverse exponential distribution with the addition of extra shape parameters which simultaneously regulates the centre and tail behaviours of the new model. The moments, fractional moments, probability weighted moment, quantile, survival and hazard rate functions, and order statistics are among the statistical characteristics of the suggested distribution that are determined and examined. The maximum likelihood estimate approach was used in a simulation exercise, and the estimator's efficiency was evaluated. The practical applicability of the model is illustrated with three real-life datasets utilizing model adequacy and goodness-of-fit measurements such as log-likelihood, Akaike information criteria, Bayesian information criteria, Kolmogorov-Smirnov (K-S) and its p-value. The data reveal that the proposed model gives a better fit than the well-known models chosen as comparators, demonstrating the EPIE distribution usefulness in medical area.

KEYWORDS

Epidemiological data, Pandemic, inverted bathtub, probability distributions.

1. INTRODUCTION

Covid-19 pandemic has underlined the crucial significance of statistical modelling in assessing and minimizing the impact of infectious disease and illness. Planning for public health, resources allocation and assessing the success of treatments all depend on accurate analysis of epidemiological datasets such as patients' survival times, recovery times and mortality rates (Overton et al. 2020). Probability distributions are fundamental tools in this endeavour as many researchers in the field of distribution theory have applied various statistical probability models to model COVID-19 datasets. Such authors include: Algarni et al. (2021), Alshanbari et al. (2022), Koobubpha et al. (2023), Almetawally (2022),

© 2026 Pakistan Journal of Statistics

Alghamdi and Abd El-Raouf (2023), Afify et al. (2022), Suleiman et al. (2023) in a bit to understanding and mitigating the impact of COVID-19 providing a mathematical framework to characterise the uncertainty and variability inherent in such data. Because classical distributions like exponential, Weibull and gamma distributions have been frequently employed in lifetime and survival studies, they typically lack the flexibility to effectively capture the complex properties of real-work scenarios (Cordeiro et al. 2013). Datasets arising from industries like health, industries and finance frequently display non-monotonic hazard rates functions like bathtub, inverted bathtub or unimodal forms which conventional models cannot capture.

Considerable efforts have concentrated on creating new and more adaptive families of probability models to overcome these constrains exhibited by the conventional models. A frequent and effective strategy is to provide additional shape parameter(s) to a baseline distribution to boost its capacity to suit a larger range of dataset structures. The exponentiation method pioneered by Gupta and Kundu (2001) is one such a powerful tool to achieve that feat. This technique builds an exponentiated family of distributions by raising the cumulative distribution function (cdf) of a baseline distribution to a positive power. This model's tweak considerably boosts the versatility and robustness of the resulting model, allowing it to capture various kinds of skewness and kurtosis and to model distinct hazard rate shapes (Nadaraja, 2005). Some of the recently developed families of probability distributions are the ones by Rannona et al. (2022) in which a new family of continuous distribution known as exponentiated odd exponential half logistic-G power series was derived. The Odd JCA-G family whose primary mathematical properties were examined by Iqbal et al. (2023) is a noteworthy contribution. El-Morshedi et al. (2022) proposed a novel Kumaraswamy-G as an alternative to class of distribution with interval (0,1). Abbas et al. (2023) derived a new Kumaraswamy-G class with a one-parameter exponential-logarithmic transformation. The Topp-Leone Gompertz-G class was created by Oluyede et al. (2022) using the distribution's extended version

Alghamdi and Abd El-Raouf (2023) proposed a new generalized family of distribution with applications to COVID-19 datasets where the model's accuracy was proved to fit the datasets better that its comparators. Moakofi and Oluyede (2023) constructed a new class of distributions known as type II exponentiated half-logistic Gompertz-G class and applied to some datasets to test its ability to fit real-life datasets. Additionally, Bhatti et al. (2023) described how the inversely related Burr X-G class derived using a T-X methodology, can fit almost any kind of failure rate. Alanzi et al. (2023) proposed new class of distribution and named it odd Muth-G utilizing the T-X approach. The authors also determined many of the model's features. Alsolami and Alsulami (2022) derived a family of distribution which can describe any complicated data, and the model was named as exponentiated-exponentiated Weibull-X family of distributions. The gamma-G class was derived by Risti-c and Balakrishnan (2012). By including two more characteristics in the odds ratio, Bourguignon and Silva (2014) developed and studied the Weibull-G class. The well-known characteristic of these generalized distributions is that they are utilized to simulate complex data structures and have more parameters. Similarly, Sule et al. (2025) introduced the exponentiated Pareto-G (EP-G) family of distributions, with probability density function (pdf) and cumulative distribution function (cdf) given as follows:

$$F(x;\pi,\kappa,\varpi)=\left[1-\left(1+H(x;\varpi)\right)^{-\pi}\right]^{\kappa} \tag{1}$$

and

$$f(x;\pi,\kappa,\varpi)=\pi\kappa h(x;\varpi)\left(1+H(x;\varpi)\right)^{-\pi-1}\left[1-\left(1+H(x;\varpi)\right)^{-\pi}\right]^{\kappa-1}. \tag{2}$$

$0\le x\le\infty$.

where $\pi,\kappa>0$ are the shape parameters and $\varpi>0$ is a vector of parameters depending on the baseline distribution used.

The inverted distributions are robust statistical distribution that their applications cut across a variety of practical disciplines, including the survival analysis in medical area, reliability theory in engineering, environmental studies, finance literature, econometrics, life testing problems, and so on. Many authors have worked on inverted distributions as a result of their wide applications such authors include: Bagci et al. (2021), Abd EL-Kade et al. (2003), Al-Dayian (2004), Flaih et al. (2012), Louzada et al. (2018), Sharma et al. (2025), Abd AL-Fattah et al. (2017), Hassan and Abd-Allah (2019), Tahir et al. (2018), Akarawak et al. (2023), Hassan et al. (2020), Baharith et al. (2014), Kargbo et al. (2023), Sule (2021), Sule et al. (2022), Ragab et al. (2022), Ramzan et al. (2022), Oguntunde et al. (2017), Ibrahim et al. (2020), Adekunle et al. (2022), Mushtaq et al. (2025), Braimah et al. (2025).

The inverse exponential (IE) distribution has cdf and pdf given respectively as:

$$H(x;\eta)=e^{-\left(\frac{\eta}{x}\right)} \tag{3}$$

and

$$h\left(x,\eta\right)=\frac{\eta}{x^{2}}e^{-\left(\frac{\eta}{x}\right)}$$
$$x\ge 0,\eta>0. \tag{4}$$

The exponentiated IE distribution is good in modelling complex lifetime data because of its interesting hazard rate shape, which can display increasing, decreasing, and reversing bathtub forms (Mushtaq et al. 2025). The popularity of generalized IE distribution stems from its capacity to overcome the drawbacks of the conventional of classical distributions such as exponential or gamma distribution which frequently fail to adequately model the complexity of real-world datasets (Alzaatreh et al. 2013).

In this research work, the characteristics of the Pareto and IE distributions are compounded using an exponentiated framework to create a new lifetime model called the exponentiated Pareto inverse exponential distribution. The Pareto distribution is known for its capacity to simulate heavy-tailed occurrences, which are commonly seen in actuarial and socioeconomic data (Hassan et al. 2020). The IE distribution is a versatile model for lifetime data particularly for events with inverted bathtub or unimodal hazard rate function (Abouammoh and Alshingiti, 2009). With emphasis on its applications to complex datasets arising from the COVID-19 pandemic, the proposed model seeks to provide a highly flexible tool for statistical analysis by integrating these distributions.

The development of the exponentiated Pareto inverse exponential (EPIE) distribution is driven by many fundamental motivations highlighted as follows:

- The main driving force is the pressing requirement for reliable statistical models for COVID-19 data analysis. Since these datasets frequently defy conventional models, a few research have emphasized the need for flexible models to describe death rates and patients' survival times (Dar et al. 2022), (Liu et al. 2021). A better option that can offer more precise insights into the dynamics of the EPIE distribution.
- There is continuous desire in statistical theory and practice for distributions that give better and greater flexibility. Standard distributions are excessively strict in their assumptions about the data's underlying structures. The EPIE distribution is intended to reflect a broader range of data behaviour such as various tail weights and hazard rate functions by combining the characteristics of the Pareto distribution and IE distribution and further improving them by exponentiation.
- The areas of statistical distribution theory will benefit greatly from this development as researchers and practitioners have more tools to work with for data analysis. The study of the EPIE distribution's theoretical qualities provides a clearer understanding of how multiple distributional components are merged to form an acceptable modelling characteristic.
- Lifetime datasets especially those related to COVID-19 can exhibit complicated properties such as large tails, skewness and non-monotonic hazard rates. As the IE distribution is appropriate for a variety of hazard shapes, the Pareto distribution excels at handling heavy-tailed datasets. Their combination under the EPIE framework is inspired by the ability to construct a single unified model capable of addressing these multiple aspects concurrently.

The study is aimed at presenting the EPIE distribution and show how effective it is as a statistical model for real-world lifetime datasets, with a focus on COVID-19 datasets. The capacity of the proposed novel EPIE model to overcome the shortcomings of simpler models gives it an advantage over its comparators. This greater flexibility results in better data modelling and wider applicability in many studies domain.

2. DERIVATION OF THE EPIE DISTRIBUTION

This section derives the EPIE distribution by utilizing the EP-G family of distributions proposed by Sule et al. (2025). The expressions for the cdf and pdf of the EPIE distribution are presented. Additionally, graphical representations of the cdf and pdf are provided, highlighting their shapes with unimodal and right-skewed across all parameter settings, with differences primarily in scale and peak location.

The EPIE model with cdf expressed in the following equation is obtained by substituting the cdf specified in equation (3) into the cdf specified in equation (1) as:

$$F(x;\pi,\kappa,\mu)=\left[1-\left[1+e^{-\left(\frac{\eta}{x}\right)}\right]^{-\pi}\right]^{\kappa} \tag{5}$$

Equation (5) is differentiated with respect to x in order to obtain the pdf of the EPIE distribution which is as follows:

$$f(x;\pi,\kappa,\eta)=\pi\kappa\frac{\eta}{x^2}e^{-\left(\frac{\eta}{x}\right)}\left(1+e^{-\left(\frac{\eta}{x}\right)}\right)^{-\pi-1}\left[1-\left(1+e^{-\left(\frac{\eta}{x}\right)}\right)^{-\pi}\right]^{\kappa-1} \quad (6)$$

$0\le x\le\infty,\ \pi,\kappa>0$ and $\eta>0$.

While there are several Pareto-based and exponentiated extensions of classical distributions such as exponentiated Pareto (EP) distribution proposed by Gupta et al. (1998) and its extension proposed by Hassan et al. (2021), the generating mechanism and parameter interaction of the proposed EPIE distribution are structurally different. In contrast to conventional exponentiated families, which alter the distribution function solely by a single power parameter, the EPIE model combines an exponentiation parameter with a Pareto-type tail adjustment, providing better control over both skewness and tail thickness at the same time. Furthermore, because of the way its three parameters interact, the EPIE model shows more hazard flexibility than many inverse exponential extensions, which maintain monotone hazard behavior. It differs from the current inverse exponential and exponentiated inverse exponential models due to this structural characteristic.

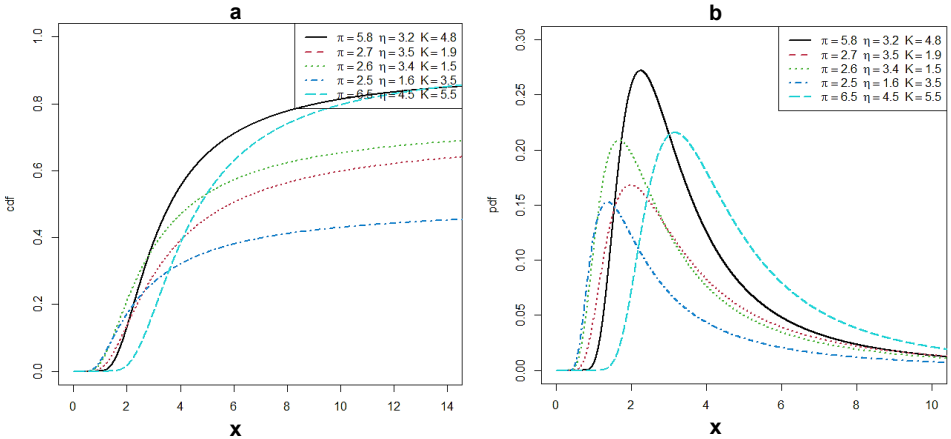

Figure 1: (a) cdf plots (b) pdf Plots of the EPIE Distribution showing Different Shapes of the Model

Figure 1 shows the cdf and pdf plots of the EPIE distribution with different values of the parameters. Figure 2(a) represents the cdf plots and it is consistent with the survival and hazard plots. Smaller value of π and η tends to shift events earlier. Larger κ tends to spread the event distribution over a long period. Figure 2(b) shows the pdf plot of EPIE distribution and how the probability of event is distributed over time. It shows the peak of a distribution where events are most likely to occur, how spread out the even times are and whether failures happen early or late. The plot rises from zero slowly to a unimodal peak where failure mostly occurred and then start declining gradually where fewer events occurred.

3. IMPORTANT REPRESENTATION OF THE DENSITY

This section presents the density expansion of the EPIE distribution as a linear representation of the EPIE distribution.

$$\left(1+\wp\right)^{-\vartheta}=\sum_{a=0}^{\infty}(-1)^{a}\binom{\vartheta+a-1}{a}\wp^{a},\ |\wp|<1 \tag{7}$$

Equation (7) is a negative binomial series expansion for any real number $\vartheta>0$.

$$\left(1-\wp\right)^{\vartheta}=\sum_{b=0}^{\infty}(-1)^{b}\binom{\vartheta}{b}\wp^{b},\ |\wp|<1 \tag{8}$$

Equation (8) is the ordinary binomial theorem if ϑ is a non-negative integer,

Binomial series expansions are represented by equations (7) and (8). They are derived from the generalized binomial theorem, which applies real (or complex) exponents to the regular binomial expansion. Using equations (7) and (8) on the last term in equation (6), the density expansion of the EPIE distribution is given as:

$$f(x;\pi,\kappa,\eta)=\pi\kappa\frac{\eta}{x^{2}}e^{-\left(\frac{\eta}{x}\right)}\left(1+e^{-\left(\frac{\eta}{x}\right)}\right)^{-\pi-1}\left[1-\left(1+e^{-\left(\frac{\eta}{x}\right)}\right)^{-\pi}\right]^{\kappa-1}$$

$$\left[1-\left[1+e^{\left(\frac{-\eta}{x}\right)}\right]^{-\pi}\right]^{\kappa-1}=\sum_{b=0}^{\infty}(-1)^{b}\binom{\kappa-1}{b}\left[1+e^{\left(\frac{-\eta}{x}\right)}\right]^{-\pi b}$$

$$\left[1+e^{\left(\frac{-\eta}{x}\right)}\right]^{-\pi(b+1)-1}=\sum_{a=0}^{\infty}(-1)^{a}\binom{\pi(b+1)+a-2}{b}\left[e^{\left(\frac{-\eta}{x}\right)}\right]^{a}$$

$$f(x;\pi,\kappa,\eta)=\pi\kappa\eta\sum_{a=0}^{\infty}\sum_{b=0}^{\infty}(-1)^{a+b}\binom{\pi(b+1)+a-2}{a}\binom{\kappa-1}{b}x^{-2}\left[e^{-\left(\frac{\eta}{x}\right)}\right]^{a+1}. \tag{9}$$

4. PROPERTIES OF THE EPIE DISTRIBUTION

This section deals with the statistical and mathematical properties of the EPIE distribution such as moments, moment generating function, probability weighted moments, quantile function, survival function and hazard rate function of the EPIE distribution.

4.1 Moments

The shape and characteristics of a pdf is described by moments and it is used to estimate the mean, variance, skewness and kurtosis. The rth moment of X is obtained by

$$\mu'_r = \int_{-\infty}^{\infty} x^r f(x)dx . \tag{10}$$

To obtain the rth moments for EPIE distribution, equation (9) is inserted into equation (10) as follows:

$$\mu'_r = \pi\kappa\eta \sum_{a=0}^{\infty}\sum_{b=0}^{\infty}(-1)^{a+b}\binom{\pi(b+1)+a-2}{a}\binom{\kappa-1}{b}\int_0^{\infty} x^{r-2}\left[e^{-\left(\frac{\eta}{x}\right)}\right]^{a+1} dx . \tag{11}$$

On solving the integral part in equation (11), the moments of the EPIE distribution is obtained as:

$$\mu'_r = \pi\kappa\eta^r \sum_{a,b=0}^{\infty}(-1)^{a+b}\binom{\kappa-1}{a}\binom{\pi(a+1)+b-2}{b}(b+1)^{r-1}\Gamma(1-r) . \tag{12}$$

When $r=1$ in equation (12), the mean of the EPIE distribution is obtained. Since the Gamma function has a pole at zero, $\Gamma(0)$ is undefined, which implies that the first moment $(r=1)$ does not exist. Consequently, higher-order moments (e.g., variance) also diverge.

4.2 Fractional Moments (fm)

A fractional moment is a moment of non-integer order in probability theory. The fm of a random variable X is defined as:

$$E\left(X^r\right) = \int_{-\infty}^{\infty} x^r f(x)dx . \tag{13}$$

From equation (6), let $u = e^{\left(\frac{-\eta}{x}\right)}, x = \frac{\eta}{\ln v}, dx = \frac{\eta}{v(\ln v)^2}dv$.

After simplification, the integral reduces to a Beta-series form using binomial expansion.

$$\left[1-\left[1+v\right]^{-\pi}\right]^{\kappa-1} = \sum_{j=0}^{\infty}(-1)^j\binom{\kappa-1}{j}\left[1+v\right]^{-\pi b}$$

$$\left[1+v\right]^{-\pi-1-\pi j} = \left[1+v\right]^{-\pi(j+1)-1}$$

After algebra and using Beta-function integrals, we obtain the fm as

$$E\left(X^r\right)=\pi\kappa\eta^r\sum_{j=o}^{\infty}(-1)^j\binom{\kappa-1}{j}B\left(1-r,\pi\left(j+1\right)+1\right). \tag{14}$$

where

$$B\left(a,b\right)=\frac{\Gamma(a)\Gamma(b)}{\Gamma(a+b)}.$$

The fractional moment exists if $r<1$.

4.3 Probability Weighted Moments (pwms)

The pwms are applied in the estimation of parameters for a probability distribution. They may also be used as starting values for maximum likelihood estimates. Given a random variable X with a cdf F, the pwms is defined to be:

$$\omega_{r,s}=E\left[X^rF(X)^s\right]=\int_0^{\infty}x^rf(x)(F(x))^s\,dx. \tag{15}$$

The pwms of the EPIE distribution is given as follows:

Denote $G(x)=1-\left[1+e^{\frac{-\eta}{x}}\right]^{-\pi}$ in equation (5).

Then, $F(x)=\left[G(x)\right]^{\kappa}$.

$$\omega_{r,s}=\int_0^{\infty}x^rf(x)\left[G(x)\right]^{\kappa s}\,dx.$$

Substitute for $f(x)$.

$$\omega_{r,s}=\pi\kappa\int_0^{\infty}x^{r-2}\eta e^{\frac{-\eta}{x}}\left[1+e^{\frac{-\eta}{x}}\right]^{-\pi-1}\left[G(x)\right]^{\kappa(s+1)-1}dx$$

Using binomila expansion, we have

$$\left[G(x)\right]^{\kappa(s+1)-1}=\sum_{j=0}^{\infty}(-1)^j\binom{\kappa(s+1)-1}{j}\left[1+e^{\frac{-\eta}{x}}\right]^{-\pi j}$$

Then,

$$\left[1+e^{\frac{-\eta}{x}}\right]^{-\pi j-\pi-1}=\left[1+e^{\frac{-\eta}{x}}\right]^{-\pi(j+1)-1}.$$

Let $u=e^{\left(\frac{-\eta}{x}\right)}$.

After transformation and simplification, the integral reduces to Beta-function form.

Therefore, the PWMs is given as

$$\omega_{r,s} = \pi\kappa\eta^{r}\sum_{j=0}^{\infty}(-1)^{j}\binom{\kappa(s+1)-1}{j}B\left(1-r,\pi(j+1)+r\right). \tag{16}$$

where $B(a,b)=\dfrac{\Gamma(a)\Gamma(b)}{\Gamma(a+b)}$, $r<1$.

4.4 Quantile Function (qf)

The qf of is crucial in statistical analysis. It computes the value in the cdf of a distribution inversely at a given probability and it serves as a cornerstone in statistical modelling. The qf of the EPIE distribution is obtained as:

$$\left[1-\left[1+e^{-\left(\frac{\eta}{x}\right)}\right]^{-\pi}\right]^{\kappa}=q$$

$$q^{\frac{1}{\kappa}}=1-\left[1+e^{-\left(\frac{\eta}{x}\right)}\right]^{-\pi}$$

$$1-q^{\frac{1}{\kappa}}=\left[1+e^{-\left(\frac{\eta}{x}\right)}\right]^{-\pi}$$

$$\left[1-q^{\frac{1}{\kappa}}\right]^{\frac{-1}{\pi}}=1+e^{-\left(\frac{\eta}{x}\right)}$$

$$e^{-\left(\frac{\eta}{x}\right)}=\left[1-q^{\frac{1}{\kappa}}\right]^{\frac{-1}{\pi}}-1$$

$$-\left(\frac{\eta}{x}\right)=\log\left\{\left[1-q^{\frac{1}{\kappa}}\right]^{\frac{-1}{\pi}}-1\right\}$$

$$x=M(q)=\frac{\eta}{-\log\left\{\left[1-q^{\frac{1}{\kappa}}\right]^{\frac{-1}{\pi}}-1\right\}}. \tag{17}$$

To obtain the median of the EPIE distribution, we set $q=0.5$ in equation (17).

4.5 Survival Function (sf)

The chance that a person or thing will live longer than a given period is represented by the sf. It gives an overview of the population's experience with survival. The sf is mathematically defined as:

$$s(x) = 1 - F(x). \tag{18}$$

The sf of the EPIE distribution is given as:

$$s(x) = 1 - \left[1 - \left[1 + e^{-\left(\frac{\eta}{x}\right)}\right]^{-\pi}\right]^{\kappa}. \tag{19}$$

4.6 Hazard Rate Function (hrf)

The hrf reflects the risk of the event occurring at a particular period, given that the individual has survived up to that time. It helps identify periods of high or low risk and it provides insight into the likelihood of failure or event occurrence across time. The mathematical representation of the hrf is:

$$\Lambda(x) = \frac{f(x)}{s(x)} \tag{20}$$

The hrf of the EPIE distribution is given as:

$$\Lambda(x) = \frac{\pi\kappa \frac{\eta}{x^2} e^{-\left(\frac{\eta}{x}\right)} \left(1 + e^{-\left(\frac{\eta}{x}\right)}\right)^{-\pi-1} \left[1 - \left(1 + e^{-\left(\frac{\eta}{x}\right)}\right)^{-\pi}\right]^{\kappa-1}}{1 - \left[1 - \left[1 + e^{-\left(\frac{\eta}{x}\right)}\right]^{-\pi}\right]^{\kappa}} \tag{21}$$

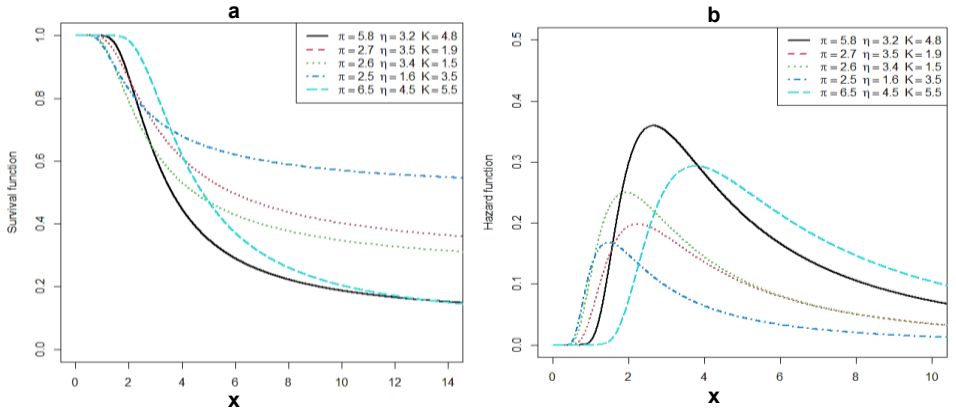

Figure 2: Plots of (a) sf and (b) hrf for the EPIE Distribution for Difference Parameter Values

Figure 2 displays the forms of the sf and hrf of the EPIE distribution with varied parameter value. The speed at which events take place is shown in Figure 2 (a) based on the parameter values. Since the hf first increases and then decreases, the survival curves fall swiftly when hf is large and flatten later when hf declines. Also, Figure 2 (b) illustrates the hrf of the EPIE model. As shown from the plot, the hrf is non-monotonic for all parameter selections that is, the hrf grows, gets to the peak and then decreases which suggests that the EPIE model has an inverted bathtub shape which is ideal in simulating medical data sets. For smaller values π and η, the peak is shifted to the left meaning that there are earlier failures. Larger values of κ tends to produce higher or more persistent hazard in the tail.

4.7 Order Statistics

In several fields such as inference and quality control, order statistics have proved crucial. It is employed in sorting the data used to deal with the application of this ordered data and their related functions (Aslam, 2023).

Order statistics are used for numerous reasons, including reliability, outlier detection, quality control, disaster planning, statistical inference, health related data analysis and goodness-of-fit assessment. Greenberg and Sarhan (1958) applied order statistics to health-related matter, Evans et al. (2006) applied the discrete random variable from order statistics in bootstrapping, Chen (2018) discussed the use of order statistics in various statistical tests and in clinical studies, Dytso et al. (2021) discussed the application of order statistics in image denoising. Bhoj and Chandra (2022) applied the order statistics for skewed distribution.

$$f_{r:n}(x) = \frac{f(x)}{B(r, n-r+1)} \sum_{v=0}^{n-r} (-1)^v \binom{n-r}{v} F(x)^{v+r-1}. \tag{22}$$

$$f_{r:n}(x) = \frac{1}{B(r, n-r+1)} \sum_{v=0}^{n-r} (-1)^v \binom{n-r}{v} \pi\kappa \frac{\eta}{x^2} e^{-\left(\frac{\eta}{x}\right)} \left(1+e^{-\left(\frac{\eta}{x}\right)}\right)^{-\pi-1}$$
$$\left[1-\left(1+e^{-\left(\frac{\eta}{x}\right)}\right)^{-\pi}\right]^{\kappa-1} \left[1-\left(1+e^{-\left(\frac{\eta}{x}\right)}\right)^{-\pi}\right]^{\kappa(v+r-1)}$$

$$f_{r:n}(x) = \frac{\pi\kappa \frac{\eta}{x^2}}{B(r, n-r+1)} \sum_{v=0}^{n-r} (-1)^v \binom{n-r}{v} e^{-\left(\frac{\eta}{x}\right)} \left(1+e^{-\left(\frac{\eta}{x}\right)}\right)^{-\pi-1}$$
$$\left[1-\left(1+e^{-\left(\frac{\eta}{x}\right)}\right)^{-\pi}\right]^{\kappa-1} \left[1-\left(1+e^{-\left(\frac{\eta}{x}\right)}\right)^{-\pi}\right]^{\kappa(v+r-1)}$$

$$f_{r:n}(x)=\frac{\pi\kappa\frac{\eta}{x^2}}{B(r,n-r+1)}\sum_{v=0}^{n-r}(-1)^v\binom{n-r}{v}e^{-\left(\frac{\eta}{x}\right)}\left(1+e^{-\left(\frac{\eta}{x}\right)}\right)^{-\pi-1}\left[1-\left(1+e^{-\left(\frac{\eta}{x}\right)}\right)^{-\pi}\right]^{\kappa(v+r)-1}$$

$$\left[1-\left(1+e^{-\left(\frac{\eta}{x}\right)}\right)^{-\pi}\right]^{\kappa(v+r)-1}=\sum_{b=0}^{\infty}(-1)^b\binom{\kappa(v+r)-1}{b}\left(1+e^{-\left(\frac{\eta}{x}\right)}\right)^{-\pi b}$$

$$\left(1+e^{-\left(\frac{\eta}{x}\right)}\right)^{-\pi(b+1)-1}=\sum_{a=0}^{\infty}(-1)^a\binom{\pi(b+1)+a-2}{a}\left(e^{-\left(\frac{\eta}{x}\right)}\right)^a$$

$$f_{r:n}(x)=\frac{\pi\kappa\frac{\eta}{x^2}}{B(r,n-r+1)}\sum_{v=0}^{n-r}(-1)^v\binom{n-r}{v}\sum_{b=0}^{\infty}(-1)^b\binom{\kappa(v+r)-1}{b}$$

$$\sum_{a=0}^{\infty}(-1)^a\binom{\pi(b+1)+a-2}{a}\left(e^{-\left(\frac{\eta}{x}\right)}\right)^{a+1}$$

$$f_{r:n}(x)=\frac{\pi\kappa\frac{\eta}{x^2}}{B(r,n-r+1)}\sum_{v=0}^{n-r}\sum_{a=0}^{\infty}\sum_{b=0}^{\infty}(-1)^{v+a+b}\binom{n-r}{v}\binom{\kappa(v+r)-1}{b}\binom{\pi(b+1)+a-2}{a}\left(e^{-\left(\frac{\eta}{x}\right)}\right)^{a+1}. \tag{23}$$

Equation (23) is the rth order statistic for the EPIE distribution.

To obtain the pdf of the minimum order statistic for the EPIE distribution, we set $r=1$ in equation (23) as:

$$f_{1:n}(x)=n\pi\kappa\frac{\eta}{x^2}\sum_{v=0}^{n-1}\sum_{a=0}^{\infty}\sum_{b=0}^{\infty}(-1)^{v+a+b}\binom{n-1}{v}\binom{\kappa(v+1)-1}{b}\binom{\pi(b+1)+a-2}{a}\left(e^{-\left(\frac{\eta}{x}\right)}\right)^{a+1}. \tag{24}$$

Also, to obtain the pdf of the maximum order statistic for the EPIE distribution, we set $r=n$ in equation (23) as:

$$f_{n:n}(x)=n\pi\kappa\frac{\eta}{x^2}\sum_{a=0}^{\infty}\sum_{b=0}^{\infty}(-1)^{a+b}\binom{\kappa(n)-1}{b}\binom{\pi(b+1)+a-2}{a}\left(e^{-\left(\frac{\eta}{x}\right)}\right)^{a+1}. \tag{25}$$

5. PARAMETER ESTIMATION

In this section, the unknown parameters are estimated using the method of maximum likelihood estimation (mle). Given that $x_1, x_2, ..., x_n$, the log-likelihood of the EPIE distribution is given as:

$$\ell(\kappa, \pi, \eta) = \sum_{i=1}^{n} \log f(x_i; \kappa, \pi, \eta) . \tag{26}$$

$$\ell(\kappa, \pi, \eta) = \sum_{i=1}^{n} \left\{ \begin{array}{l} \log + \pi \log \kappa + \eta - 2 \log x_i - \dfrac{\eta}{x_i} - (\pi + 1) \\ \log\left(1 + e^{-\left(\frac{\eta}{x_i}\right)}\right) + (\kappa - 1) \log\left(1 - \left(1 + e^{-\left(\frac{\eta}{x_i}\right)}\right)^{-\pi}\right) \end{array} \right\}. \tag{27}$$

The parameters are estimated by differentiating equation (27) and equating the results to zero. Since the equation is non-linear, an iterative technique will be used to solve them numerically using R-software.

6. SIMULATION STUDY AND APPLICATIONS

This section investigates the simulation study and real-life applications of the new model.

6.1 Simulation Study

A Monte Carlo simulation study is carried out to assess the maximum likelihood estimators' finite-sample performance. The EPIE distribution qf is used to generate R=1000 independent samples with sizes $n = 25, 50, 100, 200, 250, 300, 400, 500, 600, 700, 800$ for each parameter space $\pi = 1.5, \eta = 0.5, \kappa = 2.0$ for set I and $\pi = 0.5, \eta = 1.5, \kappa = 2.5$ for set II. The L-BFGS-B optimization technique with positive restrictions on the parameter space was used to produce parameter estimates for each replication.

Bias and Root Mean Square Error (RMSE), which are respectively defined as follows, were used to evaluate the estimators' performance:

$$Bias\left(\hat{\theta}\right) = \frac{1}{R} \sum_{r=}^{R} \left(\hat{\theta} - \theta\right)$$

$$RMSE\left(\hat{\theta}\right) = \sqrt{\frac{1}{R} \sum_{r=}^{R} \left(\hat{\theta} - \theta\right)^2}$$

where

θ is the true parameter.

$\hat{\theta}$ is the estimate from the rth replication.

R is the number of replications.

Table 1
Simulation Results for Parameters: $\pi = 1.5, \eta = 0.5, \kappa = 2.0$

Set-I				
Parameters	**n**	**MLE**	**Bias**	**RMSE**
π	25	1.6088	0.1088	0.4082
	50	1.5855	0.0855	0.3345
	100	1.5711	0.0711	0.2704
	200	1.5518	0.0518	0.2204
	250	1.5469	0.0469	0.2131
	300	1.5314	0.0314	0.2022
	400	1.5250	0.0250	0.1878
	500	1.5146	0.0146	0.1759
	600	1.5109	0.0109	0.1730
	700	1.5105	0.0105	0.1730
	800	1.5003	0.0003	0.1665
η	25	0.5243	0.0243	0.1452
	50	0.5070	0.0070	0.1026
	100	0.4981	-0.0019	0.0760
	200	0.4966	-0.0034	0.0590
	250	0.4956	-0.0044	0.0570
	300	0.4929	-0.0071	0.0524
	400	0.4915	-0.0085	0.0481
	500	0.4914	-0.0086	0.0458
	600	0.4912	-0.0088	0.0451
	700	0.4906	-0.0094	0.0426
	800	0.4902	-0.0098	0.0409
κ	25	2.2313	0.2313	0.6829
	50	2.1692	0.1692	0.5562
	100	2.1498	0.1498	0.4735
	200	2.1088	0.1088	0.3968
	250	2.1042	0.1042	0.3866
	300	2.1033	0.1033	0.3759
	400	2.1026	0.1026	0.3436
	500	2.1012	0.1012	0.3230
	600	2.0599	0.0599	0.3224
	700	2.0322	0.0322	0.3158
	800	2.0120	0.0120	0.2999

Figure 2
Simulation Results for Parameters: $\pi = 0.5, \eta = 1.5, \kappa = 2.5$

Set-II				
Parameters	**n**	**MLE**	**Bias**	**RMSE**
π	25	0.5503	0.0503	0.2970
	50	0.5325	0.0325	0.2554
	100	0.5153	0.0153	0.1826
	200	0.5152	0.0152	0.1420
	250	0.5166	0.0166	0.1320
	300	0.5108	0.0108	0.1224
	400	0.5102	0.0102	0.1058
	500	0.5078	0.0078	0.0974
	600	0.5067	0.0067	0.0888
	700	0.5064	0.0064	0.0825
	800	0.5046	0.0046	0.0784
η	25	1.8354	0.3354	0.9636
	50	1.7191	0.2191	0.7163
	100	1.6181	0.1181	0.4765
	200	1.5506	0.0506	0.3415
	250	1.5374	0.0374	0.3106
	300	1.5340	0.0340	0.2764
	400	1.5282	0.0282	0.2398
	500	1.5204	0.0204	0.2211
	600	1.5163	0.0163	0.1999
	700	1.5135	0.0135	0.1885
	800	1.5126	0.0126	0.1782
κ	25	3.0579	0.5579	1.4500
	50	2.7986	0.2986	1.0932
	100	2.6469	0.1469	0.6988
	200	2.5944	0.0944	0.5182
	250	2.5907	0.0907	0.4738
	300	2.5622	0.0622	0.4399
	400	2.5533	0.0533	0.3700
	500	2.5403	0.0403	0.3286
	600	2.5314	0.0314	0.2998
	700	2.5298	0.0298	0.2790
	800	2.5233	0.0233	0.2615

The simulation results for the EPIE distribution are shown in Tables 1 and 2. According to the simulation results, the maximum likelihood estimation (mle) method provides a reliable and accurate estimate of the unknown parameters. This is because the final estimations are rather steady and approach the true parameter values. Additionally, as the table shows, a larger sample size results in lower bias and RMSEs, which makes the mle consistent when estimating unknown parameters. Through comprehensive Monte Carlo simulations across various sample sizes and parameter configurations, the stability and robustness of the maximum likelihood estimators were evaluated. The MLEs show good finite-sample stability, according to the results. In particular, the larger the sample size, the less the empirical bias.

With increasing n, the RMSE values continuously decrease. The estimators cluster more tightly around the true parameter values as $n \to \infty$. This behavior confirms the consistency property of MLEs.

6.2 Real-life Applications

In this section, three real-world datasets relating to COVID-19 are applied to the EPIE distribution to assess its fit and flexibility. Two of the datasets is relating to mortality rate in Senegal and United Arab Emirate (UAE) and the third dataset is relating to daily confirmed COVID-19 cases in Pakistan. The EPIE distribution is compared with six other competing distributions such as Topp-Leone exponentiated inverse exponential (TLEIE) distribution by Ibrahim et al. (2020), inverse exponential (IE) distribution, Weibull (W) distribution, Kumaraswamy inverse exponential (KIE) distribution by Oguntunde *et al.* (2014), Kumaraswamy exponential (KE) distribution by Adebayo and Chukwu (2015) and exponentiated inverse exponential (EIE) distribution by Fatima and Ahmad (2017). To get the best model that fits the considered datasets, the Bayesian Information Criterion (BIC), the Akaike Information Criterion (AIC), Kolmogorov-Smirnov (K-S) and its p-value is used and the distribution that best describes the dataset is the one with the smallest value of AIC, BIC and K-S statistic. The datasets used for the analysis are presented as follows:

Dataset I

The dataset I comprises of the COVID-19 mortality rates reported in Senegal over a 31-day period, recorded between July 18, 2021, and August 17, 2021. This dataset has previously been examined by Suleiman *et al*. (2024). The datasets are presented as:

> "0.1017, 0.1179, 0.1361, 0.1720, 0.1885, 0.1867, 0.1465, 0.0904, 0.2144, 0.0883, 0.2447, 0.1207, 0.1869, 0.2504, 0.3282, 0.2271, 0.2897, 0.1437, 0.4596, 0.2817, 0.2469, 0.1528, 0.2269, 0.1954, 0.4639, 0.2820, 0.1323, 0.2334, 0.2470, 0.1882, 0.2022."

Table 3
Descriptive Statistics based on Data Set I

N	Min.	Max.	Q1	Q2	Q3	Skewness	Kurtosis	Variance	SD	Mean
31	0.0883	0.4639	0.1451	0.1954	0.2470	1.1785	4.5362	0.0083	0.0910	0.2112

Table 4
The mle Values, Negative Log-Likelihood, AIC and BIC for EPIE Model and its Comparators for Dataset I

Models	$\hat{\pi}$	$\hat{\eta}$	$\hat{\kappa}$	$-ll$	AIC	BIC	K-S	P-value
EPIE	20.7018	0.7666	0.6306	-34.9046	-63.8092	-59.5072	0.1002	0.8845
TLEIE	0.3787	0.0178	625.1239	-31.0649	-56.1298	-51.8278	0.1812	0.2311
IE	-	0.1789	-	-17.2343	-32.4685	-31.0346	0.3641	0.0003
W	-	2.4788	34.9511	-32.2013	-60.4026	-57.5346	0.1723	0.7411
KIE	0.9279	10.5476	0.5752	-34.6068	-63.2135	-58.9116	0.1088	0.8182
KE	12.9641	16.5230	0.7936	-34.5803	-63.1606	-58.8587	0.1098	0.8097
EIE	-	0.7342	0.2437	-17.2343	-30.4685	-27.6006	0.3640	0.0003

Dataset II

The dataset II represents a COVID-19 mortality rate belonging to The United Kingdom (UK) spanning from 15 October to 7 November 2020 with 24 samples. This dataset can be found in the articles by Alghamdi *et al.* (2023) and Suleiman *et al*. (2023) as they have previously reported and used the datasets. The dataset is as follows:

0.2240, 0.2189, 0.2105, 0.2266, 0.0987, 0.1147, 0.3353, 0.2563, 0.2466, 0.2847, 0.2150, 0.1821, 0.1200, 0.4206, 0.3456, 0.3045, 0.2903, 0.3377, 0.1639, 0.1350, 0.3866, 0.4678, 0.3515, 0.3232.

Table 5
Descriptive Statistics based on Data Set II

N	Min.	Max.	Q1	Q2	Q3	Skewness	Kurtosis	Variance	SD	Mean
24	0.0981	0.4678	0.2031	0.2515	0.3359	0.1619	2.2848	0.0098	0.0992	0.2608

Table 6
The mle Values, Negative Log-Likelihood, AIC and BIC for EPIE Model and its Comparators for Dataset II

Models	$\hat{\pi}$	$\hat{\eta}$	$\hat{\kappa}$	$-ll$	AIC	BIC	K-S	P-value
EPIE	1449.3382	3.0012	0.1534	-24.8813	-43.7629	-40.2284	0.0852	0.9987
TLEIE	0.1099	0.1121	283.5341	-17.6541	-29.3083	-25.7741	0.3665	0.1810
IE	-	0.2200	-	-7.9501	-13.9002	-12.7222	0.3748	0.0015
W	-	2.9595	37.8676	-22.3491	-40.6982	-38.3421	0.0960	0.9890
KIE	0.0465	11.1234	14.5450	-21.0978	-36.1955	-32.6613	0.1207	0.8350
KE	3.8268	2.0522	21.0983	-22.2536	-38.5071	-34.9730	0.0996	0.9830
EIE	-	0.2463	0.8932	-7.9501	-11.9002	-9.5441	0.3751	0.0015

Dataset III

Dataset III encompasses the daily confirmed COVID-19 cases in Pakistan, recorded from March 24 to April 28, 2020. The original dataset consists of the daily recorded confirmed cases of COVID-19 in Pakistan Al-Marzouki et al. (2020). The data spans from March 24 to April 28, 2020:

108, 102, 133, 170, 121, 99, 236, 178, 250, 161, 258, 172, 407, 577, 210, 243, 281, 186, 254, 336, 342, 269, 520, 414, 463, 514, 427, 796, 555, 742, 642, 785, 783, 605, 751, 806.

Table 7
Descriptive Statistics based on Data Set III

N	Min.	Max.	Q1	Q2	Q3	Skewness	Kurtosis	Variance	SD	Mean
36	99.00	806.00	184.00	308.50	560.50	0.5370	1.9407	54264.23	232.9468	386.00

Table 8
The mle Values, Negative Log-Likelihood, AIC and BIC for EPIE Model and its Comparators for Dataset III

Models	$\hat{\pi}$	$\hat{\eta}$	$\hat{\kappa}$	$-ll$	AIC	BIC	K-S	P-value
EPIE	63.3542	3318.2752	0.1129	-240.7305	491.0427	498.9469	0.1394	0.4463
TLEIE	17.3734	10.8222	2.8221	-244.2720	494.5440	499.2946	0.1403	0.3311
IE	-	257.805	-	-250.8568	503.7137	506.3484	0.2739	0.0071
W	-	1.7770	436.0327	-244.9984	495.9968	499.1638	0.7444	0.0099
KIE	66.8608	3.0265	7.1420	-243.5948	493.1897	496.7239	1.0000	2.2e-16
KE	0.4998	0.0447	0.0528	-250.9044	507.8089	511.3430	0.2864	0.0082
EIE	-	6.9821	36.9148	-250.8568	505.7137	508.0698	0.2737	0.0071

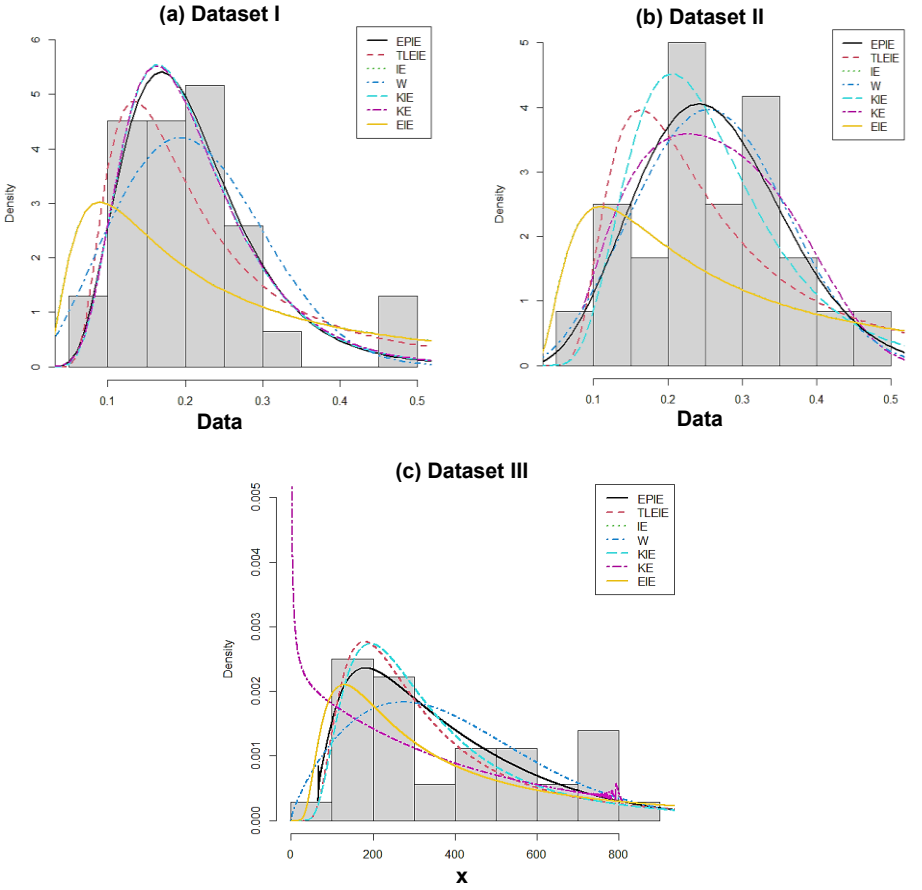

Figure 3: Histogram and Density Plots of the EPIE Distribution with its Comparators for (a) Dataset I, (b) Dataset II and (c) Dataset III

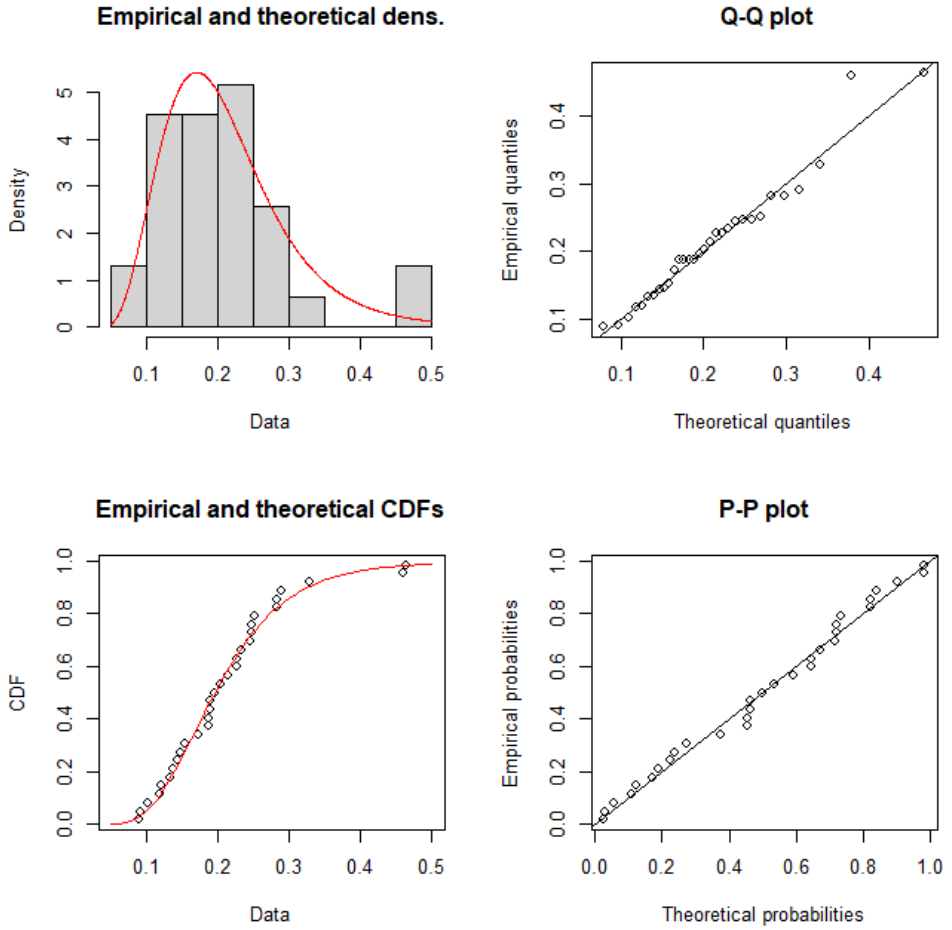

Figure 4: Theoretical, Empirical, Q-Q, and P-P Plots for EPIE Distribution for Dataset I

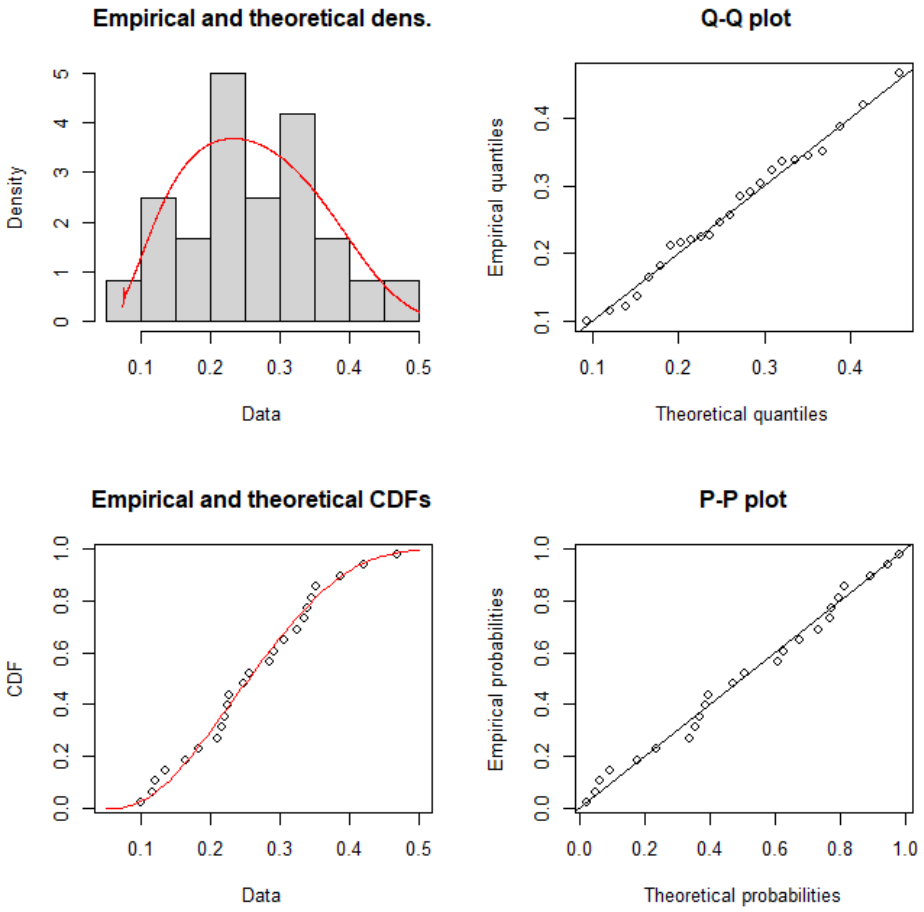

Figure 5: Theoretical, Empirical, Q-Q, and P-P Plots for EPIE Distribution for Dataset II

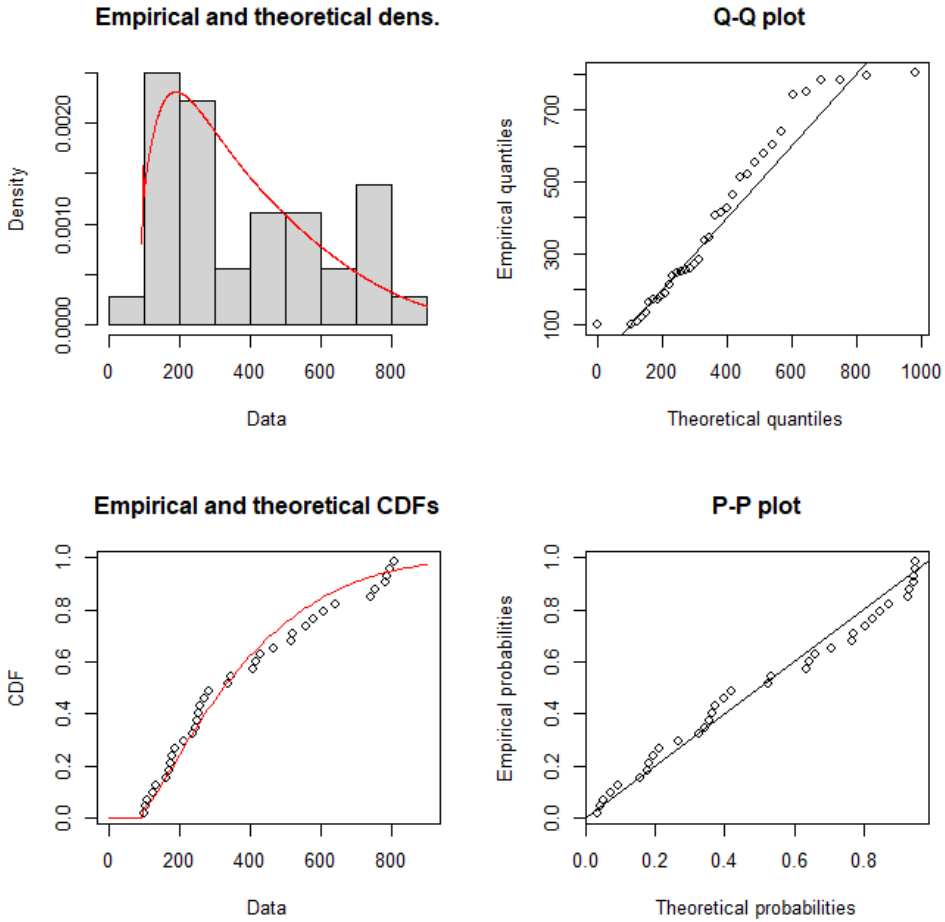

Figure 6: Theoretical, Empirical, Q-Q, and P-P Plots for EPIE Distribution for Dataset III

7. DISCUSSION OF RESULTS

Tables 3, 5 and 7 contain descriptive statistics for datasets I, II and III. From both tables, it is observed that three datasets are positively skewed data (skewness estimated to be 1.1785 for dataset I, 0.1619 for dataset II and 0.5370 for dataset III) with a heavier tail (kurtosis estimated to be 4.5362 for dataset I, 2.2848 for dataset II and 1.9407).

Tables 4, 6 and 8 present the results of the analysis using the three datasets. Tables 4 shows the results from the analysis for the dataset I and as seen from the table, the EPIE distribution has the lowest AIC, BIC and K-S values with the highest p-value, making it the best fit for the dataset I. Also, Table 6 shows the results from the analysis for the dataset II and as also seen from the table, the EPIE distribution has the lowest AIC, BIC and K-S values with the highest p-value making it the best fit the dataset II. Furthermore, Table 8 shows the results from the analysis for the dataset III, seen from the table, the EPIE

distribution has the lowest AIC, BIC and K-S values with the highest p-value making it the best fit the dataset III. These results are also supported by Figures 3, 4, 5 and 6 respectively.

Figure 3 provides the plots as histograms of datasets I, II and III with additional pdfs overlay for comparison. The purpose is to evaluate each candidate model on how well each candidate model reflects the shape, skewness and tail structure of the datasets analysed. The EPIE model is represented by the blackline in Figure 3, plot (a) pertaining to dataset I, and it most closely matches the histogram in all regions (left tail, peak, and right tail). The EPIE model also catches the skewness and tail thickness effectively. While the EIE model significantly deviates from the data in every location, the TLEIE, KIE, KE, and W models accurately capture the overall shape but differ in either the peak or the tail. As also seen from Figure 3, plot (b) relating to dataset II, the dataset has moderate skewness with a non-trivial right tail. EPIE model also provides one of the best overall fits. It closely follows the peak, right tail and left tail, smooth and well aligned with the histogram across entire support. To further buttress the applications of the EPIE model, Figure 3 (b) shows that the EPIE model has the best alignment with empirical distribution of dataset III, according to the density overlays. It correctly depicts the skewness, right-tail behavior, and modal structure. There are discernible differences in the bottom and tail portions of the KE and EIE models, while competing classical models like the Weibull and IE distributions offer adequate but less accurate fits. This is also supported in Figures 4, 5 and 6.

8. CONCLUSION

This research work introduces a new distribution called exponentiated Pareto inverted exponential distribution with real-life applications in medical science, thus increasing the flexibility of the classical inverse exponential distribution. We demonstrated its ability through the pdf, cdf, sf and hrf plots to generate various distributional shapes, including increasing, decreasing, inverted bathtub-shaped or unimodal hazard rates, making it suitable for diverse applications in reliability, survival analysis, and risk modelling. In this study, various statistical properties of the new distribution such as moments, fractional moment, probability weighted moments, quantile, survival and hazard rate functions and order statistics were derived, studied and investigated. A simulation study was conducted to determine the parameter stability of the mle approach to evaluate its performance. Datasets with inverted bathtub hazard functions, failure rates and positive skewness can all be modelled using the EPIE distribution. The novel distribution is applied to the three real-life datasets and from the results, the performance metrics used show that the EPIE model outperforms its competing distributions.

Despite its good empirical performance and demonstrated adaptability, the suggested exponentiated Pareto inverse exponential distribution has certain disadvantages. It may be vulnerable to anomalies in the data, focuses on univariate outcomes, and presupposes independent observations. Future research should extend the model to bivariate, multivariate, and time-dependent frameworks, enhance robust and Bayesian estimate methods, and carry out more exhaustive benchmarking against other heavy-tailed distributions. These developments will enhance more in-depth practical or epidemiological

interpretations of the estimated parameters and hazard behavior, theoretically and practically connecting the statistical results to public health insights.

ACKNOWLEDGEMENTS

The effort and time of the anonymous reviewers are really appreciated for their immense contribution and support in making the manuscript a standard one.

REFERENCES

1. Abbas, S., Muhammad, M., Jamal, F., Chesneau, C., Muhammad, I. and Bouchane, M. (2023). A new extension of the Kumaraswamy generated family of distributions with applications to real data. *Computation*, 11(2), DOI: 10.3390/computation11020026.
2. Abd AL-Fattah, A., El-Helbawy, A. and Al-Dayian, G. (2017). Inverted Kumaraswamy Distribution: Properties and Estimation. *Pakistan Journal of Statistics*, 33, 37-61.
3. Abd EL-Kader, R.I., AL-Dayian, G.R. and AL-Gendy, S.A. (2003). Inverted Pareto Type I distribution: properties and estimation. *Journal of Faculty of Commerce AL-Azhar University, Girls' Branch*, 21, 19-40.
4. Abouammoh, A.M. and Alshingiti, A.M. (2009). Reliability estimation of generalized inverted exponential distribution, *Journal of Statistical Computation and Simulation*, 79(11), 1301-1315.
5. Adekunle, I.K., Sule, I., Doguwa, S.I. and Yahaya, A. (2022). On the properties and applications of Topp-Leone Kumaraswamy inverse exponential distribution. *Communication in Physical Sciences*, 8(4), 590-603.
6. Adepoju, K.A. and Chukwu, O.I. (2015). Maximum Likelihood Estimation of the Kumaraswamy Exponential Distribution with Applications, *Journal of Modern Applied Statistical Methods*, 14(1), 208-214.
7. Akarawak, E.E.E., Adeyeye, S.J., Khaleel, M.A., Adedotun, A.F., Ogunsanya, A.S., Amalare, A.A. (2023). The inverted Gompertz-Fréchet distribution with applications. *Scientific African*, *21*, e01769, https://doi.org/10.1016/j.sciaf.2023.e01769
8. Afify, A.Z., Al-Mofleh, H., Aljohani, H.M. and Cordeiro, G.M. (2022). The Marshall-Olkin-Weibull-H family: Estimation, simulations, and applications to COVID-19 data. *Journal of King Saud University - Science* 34, 102115. https://doi.org/10.1016/j.jksus.2022.102115
9. Alanzi, A.R., Rafique, M.Q., Tahir, M., Jamal, F., Hussain, M.A. and Sami, W.A. (2023). A novel Muth generalized family of distributions: Properties and applications to quality control. *AIMS Math.*, 8, 6559-6580.
10. Algarni, A., Almarashi, A.M, Elbatal, I., Hassan, A.S, Almetwally, E.M., Daghistani, A. and Elgarhy, M. (2021). Type I Half Logistic Burr X-G Family: Properties, Bayesian, and Non-Bayesian Estimation under Censored Samples and Applications to COVID-19 Data. *Mathematical Problems in Engineering*, *2021*(1), 5461130. https://doi.org/10.1155/2021/5461130
11. Alghamdi, A.S. and Abd El-Raouf, M.M. (2023). Exploring the Dynamics of COVID-19 with a Novel Family of Models. *Mathematics*, 11(7), 1641, doi:10.3390/math11071641
12. Alshanbari, H.M., Odhah, O.H., Almetwally, E.M., Hussam, E., Kilai, M. and El-Bagoury, A.A.H. (2022). Novel Type I Half Logistic Burr-Weibull Distribution:

Application to COVID-19 Data. *Computational and Mathematical Methods in Medicine*, 2022(1), 1444859.
13. Almetwally, E.M. (2022). The odd Weibull inverse topp-leone distribution with applications to COVID-19 data. *Annals of Data Science*, 2022(9), 121-140.
14. Alsolami, E. and Alsulami, D. (2022). Combining Two Exponentiated Families to Generate a New Family of Distributions. *Symmetry*, 2022(14), 1739.
15. Alzaatreh, A., Lee, C. and Famoye, F. (2013). A new method for generating families of continuous distributions. *Metron*, 71(1), 63-79.
16. Aslam, M. (2023). Uncertainty-driven generation of neutrosophic random variates from the Weibull distribution, *Journal of Big Data*, (2023)10, 177. https://doi.org/10.1186/s40537-023-00860-y.
17. Al-Dayian, G. (2004). Inverted Pareto Type II distribution: Properties and estimation. *Journal of Faculty of Commerce AL-Azhar University, Girls' Branch,* 2004(*22*), 1-18.
18. Al-Marzouki, S.; Jamal, F.; Chesneau, C. and Elgarhy, M. (2020). "Erratum: Al-Marzouki, S., et al. Type II Topp Leone Power Lomax Distribution with Applications. Mathematics 2020, 8, 4". *Mathematics 8*, 871. https://doi.org/10.3390/math8060871
19. Bagci, K., Arslan, T. and Celik, H.E. (2021). Inverted Kumarswamy distribution for modelling the wind speed data: Lake Van, Turkey. *Renewable and Sustainable Energy Reviews,* 2021(135), 110110.
20. Baharith, L.A., Mousa, S.A., Atallah, M.A. and Elgayar, S.H. (2014). The beta generalized inverse Weibull distribution. *Journal of Advances in Mathematics and Computer Science*, 4(2), 252-270.
21. Bhatti, F.A., Hamedani, G., Korkmaz, M.Ç., Yousof, H.M. and Ahmad, M. (2023). On the new modified Burr XII distribution: Development, properties, characterizations and applications. *Pakistan Journal of Statistics and Operation Research,* 19, 327-348.
22. Bhoj, D.S. and Chandra, G. (2022). Ranked set sampling with varied order statistics for skew distributions. *Model Assisted Statistics and Applications,* 17(3), 161-6.
23. Bourguignon, M., Silva, R.B. and Cordeiro, G.M. (2014). The Weibull-G family of probability distributions. *Journal of Data Science*, 12(1), 53-68.
24. Braimah, J.O., Sule, I., Bello, O.A. and Correa, F.M. (2025). A New Modified Extended Generalized Inverted Exponential Distribution: A Distribution for Flexible and Accurate Data Analysis, *Contemporary Mathematics*, 6(6), 8485-8508. DOI: https://doi.org/10.37256/cm.6620257771.
25. Chen, E.J. (2018). Order statistics and clinical-practice studies. *International Journal of Computers in Clinical Practice (IJCCP)*, 3(2), 13-30.
26. Cordeiro, G.M., Ortega, E.M. and da Cunha, D.C. (2013). The exponentiated generalized class of distributions, *Journal of Data Science*, 11, 1-27. https://doi.org/10.6339/JDS.201301_11(1).0001.
27. Dar, J.G., Ijaz, M., Almanjahie, I.M., Farooq, M. and El-Morshedy, M. (2022). Statistical Analysis of the COVID-19 Mortality Rates with Probability Distributions: The Case of Pakistan and Afghanistan, *Computational and Mathematical Methods in Medicine*, 4148801, 12 pages, https://doi.org/10.1155/2022/4148801
28. Dytso, A., Cardone, M. and Rush, C. (2021). The most informative order statistic and its application to image denoising. arXiv preprint arXiv:2101.11667. 2021

29. El-Morshedy, M., Tahir, M.H., Hussain, M.A., Al-Bossly, A. and Eliwa, M.S. (2022). A new flexible univariate and bivariate family of distributions for unit interval (0, 1). *Symmetry*, 2022(14), 1040.
30. Evans, D.L., Leemis, L.M. and Drew, J.H. (2006). The distribution of order statistics for discrete random variables with applications to bootstrapping. *INFORMS Journal on Computing,* 18(1), 19-30
31. Flaih, A., Elsalloukh, H., Mendi, E. and Milanova, M. (2012). The exponentiated inverted Weibull distribution. *Applied Mathematics and Information Sciences*, 6(2), 167-171.
32. Fatima, K. and Ahmad, S.P. (2017). The Exponentiated Inverted Exponential Distribution, *Journal of Applied Information Science*, 5(1), 35-41
33. Greenberg, B.G. and Sarhan, A.E. (1958). Applications of order statistics to health data. *American Journal of Public Health and the Nations Health,* 48(10), 1388-94.
34. Gupta, R.C., Gupta, P.L. and Gupta, R.D. (1998). Modeling failure time data by Lehman alternatives. *Communications in Statistics-Theory and Methods*, 27(4), 887-904. DOI: 10.1080/03610929808832134.
35. Gupta, R.D. and Kundu, D. (2001) Exponentiated Exponential Family: An Alternative to Gamma and Weibull Distributions. *Biometrical Journal: Journal of Mathematical Methods in Biosciences*, 43, 117-130. https://doi.org/10.1002/1521-4036(200102)43:1<117::AID-BIMJ117>3.0.CO;2-R.
36. Hassan, A.S., Nassr, S.G. and Hemeda, S.E. (2020): On the extension of exponentiated Pareto distribution. *Journal of Modern Applied Statistical Methods*, 19(1), DOI: 10.22237/jmasm/1619481840
37. Hassan, A.S. and Abd-Allah, M. (2019). On the inverse power Lomax distribution. *Annals of Data Science*, 6(2), 259-278.
38. Hassan, A.S., Elgarhy, M. and Ragab, R. (2020). Statistical properties and estimation of inverted Topp-Leone distribution. *Journal of Statistics Applications & Probability,* 9(2), 319-331.
39. Ibrahim, S., Akanji, B.O. and Olanrewaju, L.H. (2020). On the extended generalized inverse exponential distribution with its applications. *Asian Journal of Probability and Statistics*. 7(3), 14-27.
40. Ibrahim, S., Doguwa, S.I., Audu, I. and Jibril, H.M. (2020). On the Flexibility of Topp Leone Exponentiated Inverse Exponential Distribution, *International Journal of Data Science and Analysis. Special Issue: Data Science*. 6(3). 83-89. doi: 10.11648/j.ijdsa.20200603.12.
41. Iqbal, T., Alfaer, N.M., Tahir, M.H., Aljohani, H.M., Jamal, F. and Afify, A.Z. (2023). Properties and estimation approaches of the odd JCA family with applications. *Concurrency and Computation: Practice and Experience*, 35(1), e7417, DOI: 10.1002/cpe.7417
42. Kargbo, M., Waititu, A.G. and Wanjoya, A.K. (2023). The alpha power exponentiated inverse exponential distribution and its application on Italy's Covid-19 mortality rate data. *International Journal of Scientific Research and Engineering Development,* 6(4), 130-139.
43. Koobubpha, K., Panitanarak, T., Domthong, P. and Panitanarak, U. (2023). The Maxwell-Burr X Distribution: Its Properties and Applications to the COVID-19 Mortality Rate in Thailand. *Thailand Statistician*, 21(2), 421-434.

44. Liu, X., Ahmad, Z., Gemeay, A.M., Abdulrahman, A.T., Hafez, E.H. and Khalil, N. (2021). Modelling the survival times of the COVID-19 patients with a new statistical model: A case study from China. *PLoS ONE*, 16(7), e0254999. https://doi.org/10.1371/journal.pone.0254999
45. Louzada, F., Ramos, P.L. and Nascimento, D. (2018). The Inverse Nakagami-m Distribution: A Novel Approach in Reliability. *IEEE Transactions on Reliability*, 67(3), 1030-1042.
46. Moakofi, T. and Oluyede, B. (2020). Type II Exponentiated Half-Logistic Gompertz-G Family of Distributions: Properties and Applications. *Mathematica Slovaca*, 73(3), 785-810.
47. Mushtaq, A., Hussain, T., Shakil, M., Ahsanullah, M. and Kibria, B.M.G. (2025). An Exponentiated Inverse Exponential Distribution Properties and Applications, *Axioms,* 14, 753. https://doi.org/10.3390/ axioms14100753
48. Nadarajah, S. (2005). Exponentiated Pareto distributions, Statistics, 39(3), 255-260, DOI: 10.1080/02331880500065488
49. Oguntunde, P.E., Adejumo, A.O. and Olowokere, E.A. (2017). On the exponentiated generalized inverse exponential distribution. In: *Transactions on Engineering Technologies: 25th World Congress on Engineering (WCE 2017)*. Vol. 1. London, UK: International Association of Engineers (IAENG); p. 80-83.
50. Oguntunde, P.E., Babatunde, O.S. and Ogunmola, A.O. (2014). Theoretical Analysis of the Kumaraswamy Inverse Exponential Distribution, *International Journal of Statistics and Applications*, 4(2), 113-116.
51. Oluyede, B., Chamunorwa, S., Chipepa, F. and Alizadeh, M. (2022). The Topp-Leone Gompertz-G family of distributions with applications. *Journal of Statistics and Management Systems,* 25(6), 1399-1423.
52. Overton, C.E., Stage, H.B., Ahmad, S., Curran-Sebastian, J., Dark, P., Das, R., Fearon, E., Felton, T., Fyles, M., Gent, N. and Hall, I. (2020). Using statistics and mathematical modelling to understand infectious disease outbreaks: COVID-19 as an example. *Infectious Disease Modelling*, 5, 409-441.
53. Ragab, M. and Elhassanein, A. (2022). A new bivariate extended generalized inverted Kumaraswamy Weibull distribution. *Advances in Mathematical Physics*, 2022(1), 1-13. https://doi.org/10.1155/2022/1243018
54. Ramzan, Q., Amar, S., Amin, M., Alshanbari, H.M., Nazeer, A. and Elhassanein, A. (2022). On the extended generalized inverted Kumaraswamy distribution. *Computational Intelligence and Neuroscience*, 2022(1), 1-18.
55. Rannona, K., Oluyede, B., Chipepa, F. and Makubate, B. (2022). The exponentiated odd exponential half logistic-G power series class of distributions with applications. *Journal of Statistics and Management Systems*, 25(8), 1821-1848.
56. Ristić, M.M. and Balakrishnan, N. (2012). The gamma-exponentiated exponential distribution. *Journal of Statistical Computation and Simulation*, 82(8), 1191-1206.
57. Sharma, V.K., Singh, S.K., Singh, U. and Agiwal, V. (2015). The inverse Lindley distribution: A stress-strength reliability model with application to head and neck cancer data. *Journal of Industrial and Production Engineering,* 32(3), 162-173.
58. Sule, I., Lawal, H.O. and Bello, A.O. (2022). Properties of a new generalized family of distributions with applications to relief times of patients' data. *Journal of Statistical Modelling and Analytics*, 4(1), 39-55.

59. Sule, I.; Bello, O.A.; Kolawole, I.A. (2025). A new Generalized Exponentiated Family of Continuous Distributions with Applications to Environmental Data Sets, *Reliability: Theory & Applications*, 1(82), 38-52.
60. Sule, B.O. (2021). A new extended generalized inverse exponential distribution: Properties and applications. *Asian Journal of Probability and Statistics*, 11(2), 30-46.
61. Suleiman, A.A., Daud, H., Singh, N.S.S., Ishaq, A.I. and Othman, M. (2023). A New Odd Beta Prime-Burr *X* Distribution with Applications to Petroleum Rock Sample Data and COVID-19 Mortality Rate. *Data*, 8(9), 143. https://doi.org/10.3390/data8090143
62. Tahir, M., Cordeiro, G.M., Ali, S., Dey, S. and Manzoor, A. (2018). The inverted Nadarajah-Haghighi distribution: Estimation methods and applications. *Journal of Statistical Computation and Simulation,* 88(14), 2775-2798.